Highly ionized iron absorption lines from outflowing gas in the X-ray spectrum of NGC 1365

G. Risaliti[1,2], S. Bianchi[3], G. Matt[4], A. Baldi[1], M. Elvis[1], G. Fabbiano[1], A. Zezas[1]

grisaliti@cfa.harvard.edu

ABSTRACT

We present the discovery of four absorption lines in the X-ray spectrum of the Seyfert Galaxy NGC 1365, at energies between 6.7 and 8.3 keV. The lines are detected with high statistical confidence (from $> 20\sigma$ for the strongest to $\sim 4\sigma$ for the weakest) in two *XMM-Newton* observations 60 ksec long. We also detect the same lines, with lower signal-to-noise (but still $> 2\sigma$ for each line) in two previous shorter ($\sim$ 10 ksec) XMM observations. The spectral analysis identifies these features as FeXXV and FeXXVI $K\alpha$ and $K\beta$ lines, outflowing with velocities varying between ~ 1000 to ~ 5000 km s^{-1} among the observations. These are the highest quality detections of such lines so far. The high equivalent widths (EW($K\alpha$) ~ 100 eV) and the $K\alpha/K\beta$ ratios imply that the lines are due to absorption of the AGN continuum by a highly ionized gas with column density $N_H \sim 5 \times 10^{23}$ cm^{-2} at a distance of $\sim$ 50–100 R_S from the continuum source.

Subject headings: Galaxies: AGN — X-rays: galaxies — Galaxies: individual (NGC 1365)

1. Introduction

Warm absorbers are common among Active Galactic Nuclei (AGNs). About half of the X-ray spectra of local bright Seyfert galaxies show evidence of a warm absorber with

[1]Harvard-Smithsonian Center for Astrophysics, 60 Garden St. Cambridge, MA 02138 USA

[2]INAF - Osservatorio di Arcetri, L.go E. Fermi 5, Firenze, Italy

[3]XMM-Newton Science Operations Center, European Space Astronomy Center, ESA, Apartado 50727, E-28080 Madrid, Spain

[4]Dipartimento di Fisica, Università degli Studi "Roma Tre", Via della Vasca Navale 84, I-00146 Roma, Italy

column densities in the range 10^{22}–10^{23} cm^{-2} (e.g., Reynolds 1997). High resolution grating observations performed with *Chandra* and *XMM-Newton* have shown that the warm absorber has a typical temperature of $\sim 10^6$ K, and, in some cases, outflowing velocities of a few 10^3 km s^{-1} (Sako et al. 2001, Kaspi et al. 2002, Krongold et al. 2003). Recently more extreme, "hot" absorbers, have been discovered through the observation of He-like and H-like iron absorption lines in several AGNs (e.g., in NGC 3783, Kaspi et al. 2002, Reeves et al. 2004, in PG 1115+080, Chartas et al. 2003, in PG 1211+143, Pounds et al. 2003, in MCG-6-30-15, Young et al. 2005).

Here we report the discovery of four strong absorption lines in each of four *XMM-Newton* observations of the Seyfert Galaxy NGC 1365, in the 6.7–8.3 keV band, which we identify as FeXXV and FeXXVI $K\alpha$ and $K\beta$ lines. NGC 1365 (z=0.0055, de Vaucouleurs et al. 1992) is an X-ray absorbed Seyfert Galaxy, with a 2–10 keV flux of the order of 0.5–2$\times 10^{-11}$ erg s^{-1} cm^{-2} (Risaliti et al. 2000, 2005, hereafter R05), which shows extreme X-ray variability: changes from reflection-dominated to transmission dominated states are observed on time scale as short as 3 weeks (R05). When in a transmission dominated state, the measured cold column density varies between ~ 1 and $\sim 5 \times 10^{23}$ cm^{-2}.

2. Data Analysis and Results

Two *XMM-Newton* (Jansen et al. 2001) observations of 60 ksec each were obtained in December 2003 and July 2004. Two shorter ($\sim$ 10 ksec) observations were obtained earlier in 2003. A spectral analysis of all these observations showed the source to be in transmission dominated state (R05). The observation log is reported in Table 1, together with the main parameters of the continuum fit which will be described in the next Section.

We reduced the EPIC PN and MOS data using the SAS 6.0 package. We extracted a spectrum from a circular region of 30" radius, and the background from nearby regions free from bright serendipitous sources. In all cases the background counts are negligible at all energies (on average $\sim$ 2% of the signal). In particular, we checked that no narrow background line[1] is present in the energy range which is most crucial for our analysis, i.e., between 6.7 and 8.3 keV, where the absorption lines are detected. The data obtained with the two MOS were merged. Calibration matrices were computed for each spectrum. We rebinned the spectra in order to have at least 20 counts per bin. This allows us to use χ^2 minimization in the model fitting.

[1]e.g., from Ni, Cu, Zn, see http://xmm.vilspa.esa.es/external/xmm_user_support/documentation/uhb/node35.html (Lumb et al. 2002).

For all four spectra a good fit is obtained with a model consisting of an absorbed power law with N_H between 1 and 5×10^{23} cm^{-2}, plus a cold reflection component (using the PEXRAV model in XSPEC, Magdziarz & Zdziarski 1995) and a narrow emission line at 6.4 keV. At energies below the photoelectric cut-off a thermal emission component dominates, with $kT \sim 0.8$ keV (R05). A broad emission line, probably relativistic, is also needed to properly fit the 4–6 keV region[2]. In addition to these "standard" components, four absorption lines in the energy range 6.7–8.3 keV are strongly requested by the fit. A complete analysis of the emission spectrum of NGC 1365 will be presented elsewhere, together with a detailed study of the spectral variability during the two long observations. Here we concentrate on the most striking features in these spectra, i.e., the group of absorption lines present in the 6.7–8.3 keV spectral region. In order to visually show the relevance of these lines, in Fig. 1 we plot the 5–10 keV residuals to a model with the same components as above, except for the four absorption lines, and fitted ignoring the energy ranges 6.7–7.2 keV and 7.8–8.3 keV. The spacing of the lines strongly suggests that they are FeXXV and FeXXVI $K\alpha$ and $K\beta$.

Accordingly, in the global 0.5–10 keV fits the four lines were fitted with narrow Gaussians, with free energies allowed for each single line and each single fit. All the four lines are significantly detected in all spectra, except in two cases where the detection is marginal (FeXXV Kβ in OBS 1 and OBS 2). For the two highest quality observations, OBS 3 and OBS 4, the fits were performed on PN and MOS data separately.

Since the best fit energies are close to those of the four lines mentioned above, we estimated the blueshift/redshift velocities corresponding to the differences between the measured and theoretical energies for these lines. The velocities are shown in Fig. 2. In both observations the results are in agreement with a common outflow velocity for the four lines. Therefore, we performed a new fit fixing the energies of the four lines to the theoretical values (taking into account for the redshift of the source), and allowing for a single free redshift/blueshift. We obtained as good a fit as in the previous case where all the lines were left free ($\Delta(\chi^2) < 8$ in the global fit in all observations, with three less free parameters).

The best fit line parameters are listed in Table 2. The continuum parameters, listed in Table. 1, are typical of X-ray spectra of obscured, Compton-thin Seyfert galaxies, and will be discussed in detail in a forthcoming paper.

In Fig. 3 we show the 5-10 keV spectrum and best fit model for the two long observations. The measured $K\alpha/K\beta$ ratios (Table 3) are significantly smaller than those expected from

[2]Alternative continuum models are possible, for example with the inclusion of partial covering. Here we do not investigate this point since we are only interested in an analytic fit to the continuum, in order to have a correct determination of the narrow absorption lines parameters.

the oscillator strengths ratios[3].

In all four spectra the lines are blueshifted with respect to the expected theoretical line energy peaks. The velocity shifts are between 1,000 and 5,200 km s^{-1} (Table 2), and are statistically highly significant, except for the first observation, where the data are in agreement with zero velocity. The differences between the outflow velocities are highly significant, and cannot be due to instrumental effects. In order to check the reality of this shift, we compared the low energy thermal emission lines in the ~ 1 keV region (which are expected to be constant, given the good S/N and the extent of the thermal emission region resolved by *Chandra*, R05) and found that they overlap perfectly ($\Delta(E) < 10$ eV).

3. Discussion

The main results of our spectral analysis are the following:
• We detected four absorption lines in the energy range 6.7–8.3 keV in four *XMM-Newton* observations of NGC 1365, with equivalent width in the 50-150 eV range. We identified these lines as FeXXV and FeXXVI $K\alpha$ and $K\beta$.
• In all observations the lines are blueshifted. Blueshift velocities are the same for all lines in the same observation, but vary among the different observations from $\sim 1,000$ to $\sim 5,000$ km s^{-1}.
• The $K\alpha/K\beta$ ratios are much smaller than the theoretical oscillator strength values (Table 3), and are consistent with staying constant between the observations.

In the following we discuss the composition (ionization state, column density), the geometrical structure, and origin of the hot absorber.

Composition. The low $K\alpha/K\beta$ ratios can only be explained if saturation effects are significant. Any other physical explanation is ruled out, since (a) the theoretical ratio is well established, since it involves transitions to the fundamental level in relatively simple (He-like and H-like) atomic species, and (b) the energy difference between the lines is too small for the continuum slope to play a significant role: for a photon index $\Gamma = 2.0$ we have $F_E(6.7\ \mathrm{keV})/F_E(7.9\ \mathrm{keV}) = 1.17$. Following B05, an equivalent width of the $K\alpha$ lines EW$\sim$100–150 eV can be obtained with $N_H > 10^{23}$ cm^{-2}, a turbulent velocity of the absorbing gas $v_t = 1,000$ km s^{-1}, and an ionization parameter $\log U_X = 0$.[4] We note that the EPIC

[3]Throughout this paper we refer to the atomic physics values of the NIST Atomic database (http://physics.nist.gov), and reported in Table 1 of Bianchi et al. 2005, hereafter B05.

[4]We adopt the definition in B05: $U_X = (\int_2^{10} \frac{L_\nu}{h\nu} d\nu)/(4\pi r^2 c n_e)$, similar to the one first introduced by

resolution at 8 keV corresponds to velocities of $\sim 5,000$ km s^{-1}. With the available statistics we find that the minimum detectable velocity is of the order of 2,000 km $^{-1}$. Therefore, no useful constraint on v_t can be obtained from our fits.

We calculated the curve of growth for the $K\beta$ lines using the same model as B05. In order to have a precise estimate of the EW ratios, we also considered the contribution of the FeXXV $K\gamma$ line at 8.29 keV, which is blended with the FeXXVI $K\beta$ in low resolution spectra, and has an oscillator strength about half of that of the FeXXVI $K\beta$. A further minor contribution could come from the NiXXVII (He like) $K\alpha$ at 7.98 keV. Its oscillator strength is 0.19 that of FeXXV $K\beta$. An overabundance of nickel could make this contribution important. However, we note that in this case the line profile would be significantly altered, given that the energy separation between the two lines ($\Delta E = 80$ eV) is comparable to the EPIC resolution ($\sim$ 150 eV for both PN and MOS cameras; but note that with the high statistics available the peak energies of the lines is determined with a much better precision, $\sim$10–15 eV). This is not observed (Fig. 1). We conclude that the contribution of nickel lines cannot be significant. In Fig. 4 we plot the curve of growth for the FeXXV and FeXXVI $K\alpha$ lines (from B05) and the $K\alpha/K\beta$ ratio. Note that both the large EWs and the low $K\alpha/K\beta$ ratios require an absorber with a column density $N_H \sim 5 \times 10^{23}$ cm^{-2} and a turbulent velocity $\sigma \sim$500–1,000 km s^{-1}. The right panels of Fig. 4 show the importance of saturation effects in the $K\alpha/K\beta$ ratios. High column densities are required in order to reproduce the small observed ratios.

The above estimates are computed adopting a fixed ionization parameter U_X. Therefore we expect they slightly change for different choices of U_X. However we do not expect to find acceptable solutions for significantly lower or higher ionization parameters: if (a) $\log U_X >> 0$ the iron atoms are almost completely stripped, making impossible to obtain as high EWs as observed; if (b) $-1 < \log U_X < 0$ the He-like Fe atoms are overabundant with respect to the H-like ones, because the ionizing continuum is enough to strip all the L shell electrons, but not to strip the 2 inner electrons. The ratio between FeXXV and FeXXVI lines would then be much higher than observed. This argument is discussed in more detail in B05.

The turbulent velocity is significantly higher than the thermal velocity of a gas with the same ionization state ($\sigma_T \sim$100–200 km s^{-1}). As a consequence, the line widths probably indicate true bulk motions. These might be related to the observed changes in outflow velocity.

Geometrical properties. The high ionization parameter required to explain the line

---

Netzer (1996). For ease of comparison, if $\log U_X = 0$, the ionization parameter defined as $U'_X = L_X/(n_e r^2)$ has a value $U'_X \sim 5,000$ (for an ionizing continuum with $\Gamma = 2$).

ratios can be used to put constraints on the distance of the line absorber from the X-ray continuum source, assuming that the ionization state is due to UV radiation from the central source, rather than to a high thermal temperature of the gas. For $\log U_X = 0$, $N_H = 5 \times 10^{23}$ cm^{-2}, and a 2–10 keV photon index $\Gamma = 2$ we obtain $R \sim 2 \times 10^{15}$ $(\Delta R/R)$ L_{42} cm, where L_{42} is the 2–10 keV luminosity in units of 10^{42} erg s^{-1} (Table 1) and ΔR is the thickness of the absorber along the radial direction. R is the average distance of the absorber, so we expect $\Delta R/R \sim 1$. We note that a distance of $\sim 10^{15}$ cm is of the order of what a gas with a velocity $v \sim 4,000$ km s^{-1} (intermediate between the two measurements in the last two observations, OBS 3 and OBS 4) would cover in ~ 6 months between OBS 3 and OBS 4 ($\sim 2 \times 10^7$ sec). This is in qualitative agreement with our assumption of an absorbing gas with a thickness of the same order of the distance from the central source. A smaller thickness ($\Delta R/R < 1$) would imply an even smaller distance from the central source.

Origin. The short distance inferred from the high ionization state of the absorber, and the rough black hole mass estimate ($M_{BH} \sim 10^8$ $M_\odot$, R05) imply that the gas is located at the radii of the accretion disk, ~ 50 $(M/M_8)^{-1}$ Schwarzschild radii from the black hole. Hot gas could be present in this region either as the external part of the hot corona believed to be responsible of the X-ray emission in AGNs[5] (e.g., Haardt & Maraschi 1991), or as the inner part of a wind arising from the disk (Murray & Chiang 1995, Proga et al. 2000).

We note that the observed blueshift velocity is smaller than the escape velocity at 50 $(M/M_8)^{-1} R_S$, which is of the order of about 50,000 $(M/M_8)^{-0.5}$ km s^{-1}. However, the observed velocity is of the order of that predicted in the vertical part of the funnel-shaped wind of Elvis (2000). The main problem with the wind scenario is that radiation force in not an effective acceleration mechanism in our case, since the gas is overionised (so line absorption is not an efficient way to transfer momentum from radiation to gas) and the bolometric luminosity (of the order of a few 10^{43} erg s^{-1} adopting a standard X-ray to bolometric correction, Risaliti & Elvis 2004) is a small fraction of the Eddington luminosity, $L_{EDD} \sim 2 \times 10^{46} (M/M_8)^{-1}$ erg s^{-1}, making Thomson scattering acceleration negligible with respect to gravity. However, two mechanisms could provide the observed highly ionized gas: (a) a poloidal magnetic field could effectively extract the gas from the accretion disk and form a wind (Blandford & Payne 1982, Konigl & Kartje 1994); (b) gas arising from the accretion disk due to local instabilities would be ionized by the central UV/X-ray source, and initially expand towards the vertical direction (with respect to the disk plane) due to its internal pressure. The gas would then fail to form a wind if no external force is present, but a fraction of the line of sight, at small angles with respect to the disk plane, would be covered

[5]The inner corona, emitting the bulk of X-ray radiation, has to have $kT \sim 100$ eV, therefore it is too hot to absorb its own radiation.

by such gas, with the required ionization state and column density, and with a (temporary) outflowing velocity of the order of a few 10^3 km s^{-1}. Similar properties are predicted for the inner "hitchhiking gas" in radiation driven wind models (Murray & Chiang 1995).

We are grateful to F. Nicastro and N. Brickhouse for useful discussions. This work was partially supported by NASA grants NAG5-13161, NNG04GF97G, and NAG5-16932.

REFERENCES

Bianchi, S., Matt, G., Nicastro, F., Porquet, D., & Dubau, J. 2005, MNRAS, 357, 599 (B05)

Blandford, R. D., & Payne, D. G. 1982, MNRAS, 199, 883

Chartas, G., Brandt, W. N., & Gallagher, S. C. 2003, ApJ, 595, 85

de Vaucouleurs, G., de Vaucouleurs, A., Corwin, H. G., Buta, R. J., Paturel, G., & Fouque, P. 1992, VizieR Online Data Catalog, 7137, 0

Elvis, M. 2000, ApJ, 545, 63

Haardt, F., & Maraschi, L. 1991, ApJ, 380, L51

Jansen, F., et al. 2001, A&A, 365, L1

Kaspi, S., et al. 2002, ApJ, 574, 643

Krongold, Y., Nicastro, F., Brickhouse, N. S., Elvis, M., Liedahl, D. A., & Mathur, S. 2003, ApJ, 597, 832

Konigl, A., & Kartje, J. F. 1994, ApJ, 434, 446

Lumb, D. H., Warwick, R. S., Page, M., & De Luca, A. 2002, A&A, 389, 93

Magdziarz, P. & Zdziarski, A. A. 1995, MNRAS, 273, 837

Murray, N., & Chiang, J. 1995, ApJ, 454, L105

Pounds, K. A., King, A. R., Page, K. L., & O'Brien, P. T. 2003, MNRAS, 346, 1025

Proga, D., Stone, J. M., & Kallman, T. R. 2000, ApJ, 543, 686

Reeves, J. N., Nandra, K., George, I. M., Pounds, K. A., Turner, T. J., & Yaqoob, T. 2004, ApJ, 602, 648

Reynolds, C. S. 1997, MNRAS, 286, 513

Risaliti, G., Maiolino, R., & Bassani, L. 2000, A&A, 356, 33

Risaliti, G., & Elvis, M. 2004, ASSL Vol. 308: Supermassive Black Holes in the Distant Universe, 187

Risaliti, G., Elvis, M., Fabbiano, G., Baldi, A., & Zezas, A. 2005, ApJ, 623, L93

Sako, M., et al. 2001, A&A, 365, L168

Young, A.J., et al. 2005, ApJ, accepted (astro-ph/0506082)

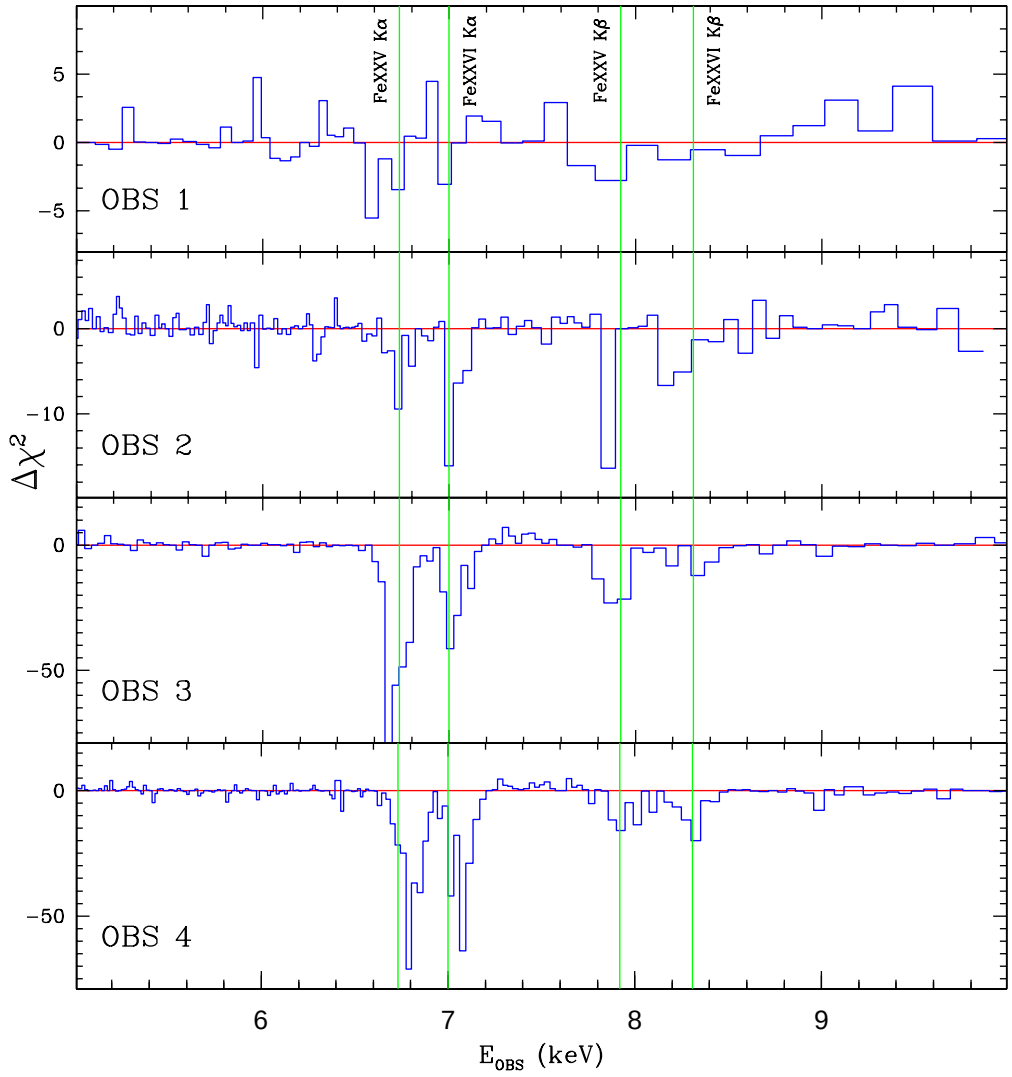

Fig. 1.— Contributions to χ^2 in the 5-10 keV range for the four MOS observations of NGC 1365. The continuum model has been fitted ignoring the energy intervals 6.7-7.2 keV and 7.8-8.3 keV. The four vertical lines show the rest frame energy of the four lines FeXXV Kα, FeXXVI Kα, FeXXV Kβ, FeXXVI Kβ.

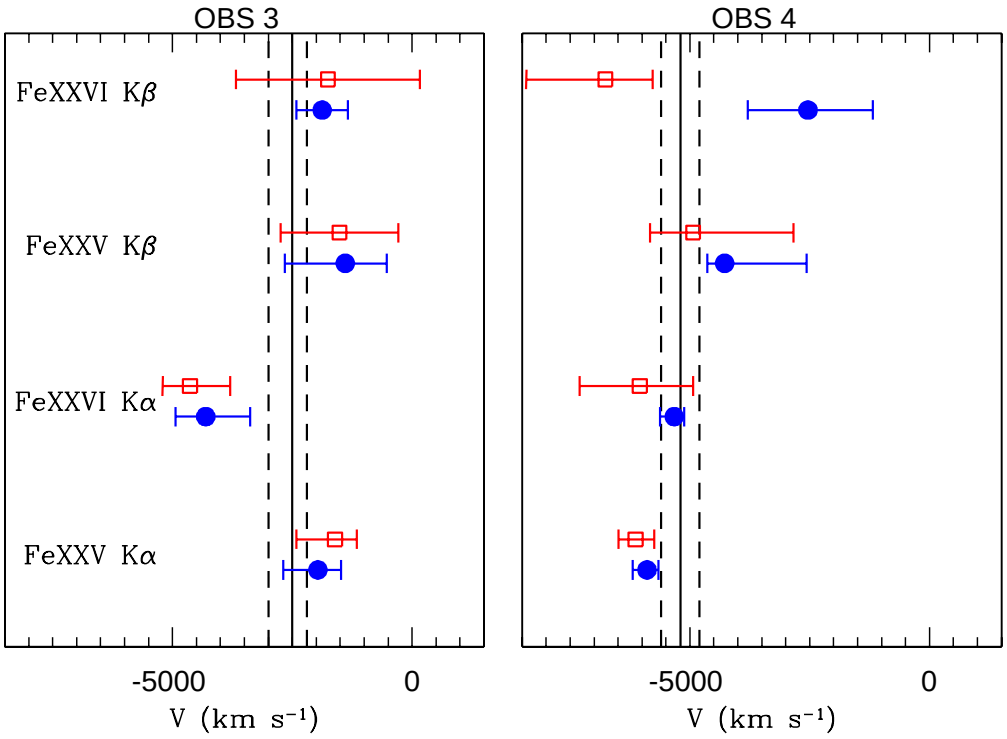

Fig. 2.— Best fit velocities for the four iron absorption lines in the two highest quality observations, OBS 3 and OBS 4. For each line we separately plot the results from the PN spectra (blue circles) and the MOS spectra (red squares). The vertical solid line shows the best fit value obtained requiring a common velocity for the four lines with $\pm 1\ \sigma$ values shown as vertical dashed lines.

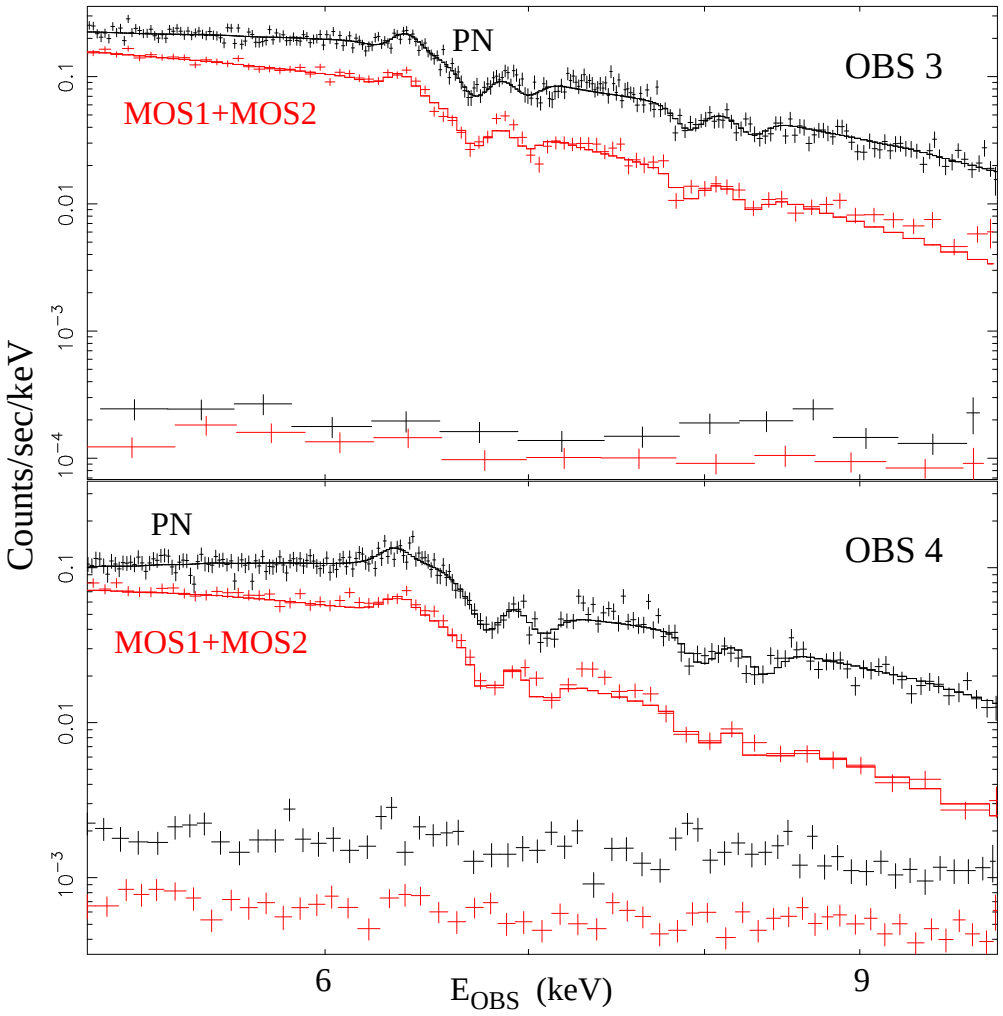

Fig. 3.— Hard X-ray (5-10 keV) spectra and best fit model for the two long *XMM-Newton* observations of NGC 1365. The background spectrum is shown for each observation.

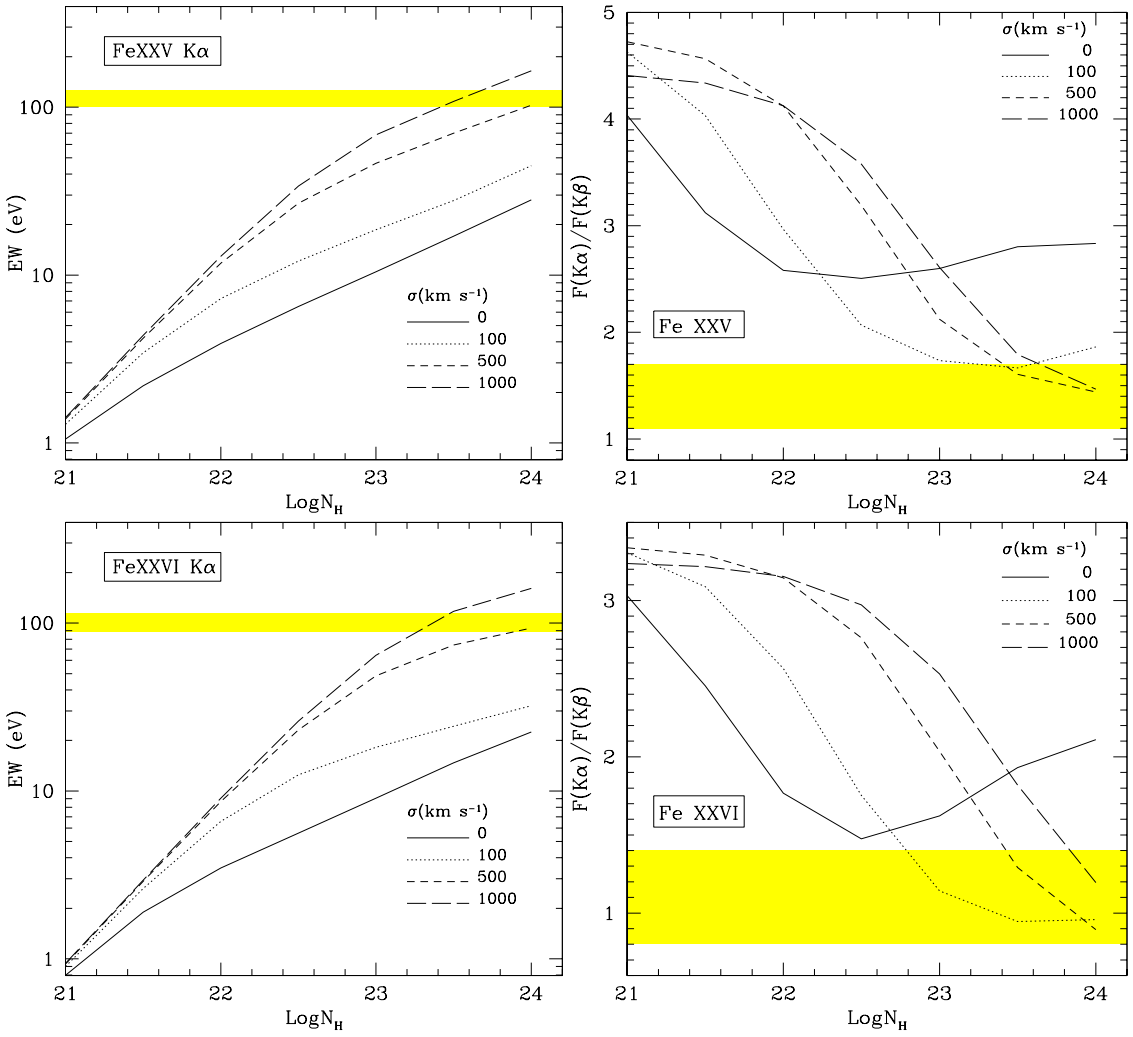

Fig. 4.— Left panels: curves of growth for the FeXXV and FeXXVI $K\alpha$ lines, for $\log U_X = 0$. Right panels: $K\alpha/K\beta$ ratios for FeXXV and FeXXVI. The yellow shaded regions are the 90% confidence intervals for the averages obtained from the four observations.

Table 1: Observation Log and Spectral Parameters

OBS	Date	t[a]	Counts[b]	F[c]	L[d]	Γ	N_H[e]
1	2003 Jan 16	14.8	14866	0.48	1.0	$2.15^{+0.03}_{-0.06}$	51^{+3}_{-3}
2	2003 Aug 13	7.1	9466	0.73	1.4	$2.32^{+0.12}_{-0.02}$	37^{+2}_{-2}
3	2004 Jan 17	59	121967	1.37	1.7	$2.55^{+0.05}_{-0.03}$	$16.3^{+0.2}_{-0.2}$
4	2004 Jul 24	60	74056	0.76	0.8	$2.11^{+0.03}_{-0.04}$	$29.4^{+0.3}_{-0.3}$

[a]Net observing time in ksec.

[b]Source counts in the 0.5-10 keV interval.

[c]2-10 keV observed flux, in units of 10^{-11} erg s^{-1} cm^{-1}.

[d]Intrinsic 2-10 keV luminosity in units of 10^{42} erg s^{-1}.

[e]In units of 10^{22} cm^{-2}.

Table 2: NGC 1365 - Data on absorption lines

Line	E(keV)	OBS 1		OBS 2		OBS 3		OBS 4	
		EW (eV)[a]	$\Delta(\chi^2)$[c]	EW (eV)[a]	$\Delta(\chi^2)$[c]	EW (eV)[a]	$\Delta(\chi^2)$[c]	EW (eV)[a]	$\Delta(\chi^2)$[c]
FeXXV $K\alpha$	6.697	110^{+45}_{-70}	17	135±30	30	120±20	173	154±20	264
FeXXVI $K\alpha$	6.966	94^{+50}_{-50}	11	111±30	20	104^{+15}_{-20}	52	145^{+15}_{-20}	167
FeXXV $K\beta$	7.880	81±55	5	100±60	6	93±10	43	108±20	60
FeXXVI $K\beta$[d]	8.268	127±60	12	130±60	10	80±15	18	110±25	59
V(km s^{-1})[b]		1000^{+1000}_{-1500}		2000^{+1800}_{-400}		2500^{+500}_{-300}		5200^{+400}_{-400}	

[a] Errors are at a 90% confidence level.

[b] Outflowing velocity of the absorbing gas.

[c] $\Delta(\chi^2)$ with respect to the best fit model without the four absorption lines. The four lines are forced to have the same blueshift, so the model including the lines has 5 more parameters than the no-line model.

[d] The FeXXVI $K\beta$ line is blended with the FeXXV $K\gamma$ (see text for details).

Table 3: FeXXV and FeXXVI $K\alpha/K\beta$ ratios

	OBS 1	OBS 2	OBS 3	OBS 4	R^a_{AV}	Th.^{b}
FeXXV	1.4±1.7	1.4±1.1	1.4±0.4	1.4±0.4	1.4±0.3	5.0
FeXXVI	0.7±0.7	0.9±0.6	1.4±0.7	1.3±0.4	1.1±0.3	3.2

^{a}: Average ratios: ^{b}: Oscillator strengths ratio. In R2 the contribution of FeXXV Kγ has been taken into account.